

BEAM DIAGNOSTICS OF THE LIPAC INJECTOR WITH A FOCUS ON THE ALGORITHM DEVELOPED FOR EMITTANCE DATA ANALYSIS OF HIGH BACKGROUND INCLUDING SPECIES FRACTION CALCULATION

B. Bolzon[#], N. Chauvin, S. Chel, R. Gobin, F. Senée, M. Valette, CEA, Gif-sur-Yvette, France
 K. Shinto, JAEA, Rokkasho Fusion Institute, Rokkasho, Japan
 J. Knaster, Y. Okumura, IFMIF/EVEDA Project Team, Rokkasho, Japan

Abstract

To prove the technical feasibility of the IFMIF accelerators concept, the EVEDA phase will commission in Japan the LIPAC accelerator, which will deliver a 125 mA/9 MeV CW deuteron beam. LEDA already managed 100 mA in CW at 6.7 MeV in 2000. The different subsystems of LIPAC have been designed and constructed mainly by European labs with the injector developed by CEA-Saclay. This injector must deliver a 140 mA/100 keV CW deuteron beam at 99% D⁺ ratio, which is produced by a 2.45 GHz ECR ion source. The low energy beam transport line (LEBT) is based on a dual solenoid focusing system to transport the beam and to match it into the RFQ. The normalized RMS target emittance at the RFQ entrance is targeted to be within 0.25 π mm·mrad. This article describes the diagnostics installed in the LEBT to measure beam parameters such as intensity, profile, emittance, species fraction and degree of space charge compensation. The article also focuses on the algorithm developed to analyze emittance data of high background from an Allison scanner. Species fractions (D⁺, D₂⁺, D₃⁺) using mass separation technique were also calculated during the on-going commissioning campaign with the Allison scanner installed between the two solenoids in a first stage.

INTRODUCTION

The IFMIF project (International Fusion Materials Irradiation Facility) will generate a neutron flux of 10¹⁸ m⁻²s⁻¹ with a broad energy peak at 14 MeV in order to characterize and study candidate materials for future fusion reactors. To reach such a challenging goal, two parallel deuteron accelerators of 5 MW each will deliver a high intensity D⁺ beam of 2 x 125 mA CW (Continuous Wave) at 40 MeV against a liquid lithium target [1]. In the present final phase before construction, called EVEDA (Engineering Validation and Engineering Design Activities), a 125 mA/9 MeV CW deuteron demonstrator accelerator called LIPAc (Linear IFMIF Prototype Accelerator) is being assembled, commissioned and will be operated in Rokkasho [2, 3]. LIPAc has been designed and constructed mainly in European labs with participation of JAEA in the RFQ couplers. It is composed of a deuteron injector delivered by CEA-Saclay [4], a Radio Frequency Quadrupole (RFQ) [5] to be delivered by INFN, eight superconducting half-wave resonators (SRF Linac) designed by CEA-Saclay [6],

Medium and High energy beam transfer lines and a beam dump designed by CIEMAT.

The injector is composed of a 2.45 GHz ECR ion source based on the CEA-Saclay SILHI source design [7] and a LEBT line that will transport and match the beam into the RFQ. After acceptance tests performed at CEA-Saclay [8, 9], it has been shipped to Japan in 2013 and is currently under commissioning in Rokkasho [10, 11]. According to requirements, the D⁺ beam injected into the RFQ must be 140 mA/100 keV CW with a normalized RMS emittance lower than 0.30 π mm·mrad (with a target value of 0.25 π mm·mrad). Under these conditions, simulations demonstrated that the deuteron beam can be accelerated to 5 MeV by the RFQ with less than 10% losses in order to reach the specified 125 mA CW. This paper details the different beam diagnostics available in the LEBT, not only during this commissioning phase, but also during operation. A particular focus is made on the validation of the algorithm developed to analyze data of high background from an Allison scanner in order to compute emittance and determine species fraction ratio (D⁺, D₂⁺, D₃⁺) extracted from the ion source.

BEAM DIAGNOSTICS IN THE LEBT

The LEBT consists of an accelerator column (containing the ion source extraction system), two solenoids with integrated H/V steerers, a diagnostic box located between the solenoids and an injection cone located just upstream the RFQ. During the injector commissioning, a specific diagnostic box, equipped with a beam stopper designed to handle a 15 kW beam, is placed after the injection cone. To minimize the emittance growth driven by the high beam space charge, the LEBT length has been minimized to 2.05 m from the plasma electrode to the internal face of the RFQ entrance. In such a short line and due to the radiation environment induced by the D-D fusion reactions from beam losses and deuterium adsorbed in the beam pipe walls, only few diagnostics can be installed: Charge Injection Device (CID) cameras, a deuterated spectrometer beyond the shielding walls via a radiation hardened optical fiber, an Allison scanner, a Four Grid Analyser, an ACCT and a movable beam stopper have been selected to characterize the beam during commissioning and operation.

A 3D view of the LIPAc injector with its dedicated beam diagnostics is shown on Fig. 1.

[#]benoit.bolzon@cea.fr

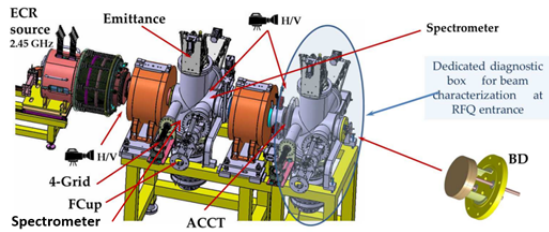


Figure 1: Scheme of the LIPAc injector with its dedicated beam diagnostics.

Beam Current Measurement

The total current extracted from the ECR source (including D^+ , D_2^+ and D_3^+ ion species) is provided with an error of a few percent by the output current flow of the main high-voltage power supply. The beam current can also be estimated between the two solenoids thanks to a movable beam stopper which is initially used to protect the valve isolating the LEBT vacuum from the rest of the system (for space optimization reasons, the sector valve is placed between both solenoids). At the end of the LEBT, the beam current can be measured with an ACCT (AC Current Transformer) located at the end of the injection cone and with the beam stopper located inside the diagnostic box. The ACCT, capable of measuring pulsed beams above few microseconds, will allow estimating the current transmission of the RFQ by comparison with another ACCT located at the beginning of the MEBT. A DCCT (DC Current Transformer) would have obviously been preferable for CW operation but space constrains, driven by space charge induced emittance growth, were in place.

Improvement of Beam Stoppers Measurements

In high intensity and low energy beam lines, the interaction of charged particles with a beam stopper (metallic surface) induces the production of secondary electrons (from few tens of eV to 100 eV) and overestimations of the beam current measurements can take place (see Fig. 2). This potential difficulty has been partly solved in LIPAc injector by an auto-polarization of the beam stopper; however, this polarization induces the attraction of electrons which are trapped into the beam (in turn, allowing the space charge compensation) and of secondary electrons emitted by the beam losses hitting the beam pipe. In these cases, the real current is underestimated unavoidably given the subtracting contribution of the electrons in the measurement values.

A study of a dipolar magnetic system is planned to be done in order to remove the contribution of secondary electrons on the current measurements. Two solutions can be considered: 1) a dynamic and adjustable dipole or 2) a static dipole by means of a permanent magnet, which is perceived as simpler and substantially cheaper. In the case of the movable beam stopper, the permanent magnets may slightly deflect the primary beam when the equipment would be pulled out; at the same time, the power supply of a dynamic dipole can be cut off when the beam stopper is pulled out. A static dipole can thus be considered for

the beam stopper installed at the end of the LEBT, while a dynamic dipole has to be designed for the movable beam stopper installed between the two solenoids.

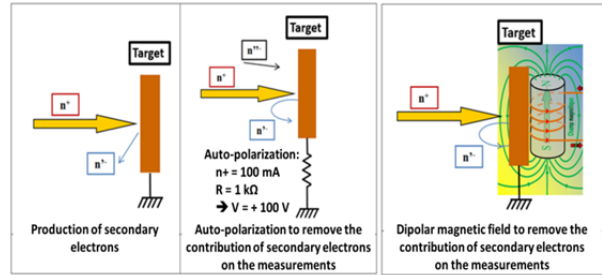


Figure 2: Suppression of the contribution of secondary electrons on current measurements with a beam stopper.

Optical Beam Diagnostics

In the LEBT of LIPAc, optical diagnostics based on the fluorescence of residual gas are used to characterize the high intensity ion beam [12, 13]. These devices are radiation hardened since high neutron and gamma rays flux are emitted when operating the LEBT with deuterons; in that case, even activation of materials will take place [9].

Four CID cameras (radiation hardness up to ~ 30 kGy), known to be more resistant to radiation than more usual Coupled Charge Device (CCD) cameras, have been installed perpendicularly to the beam direction in the LEBT in order to measure both horizontal and vertical profiles at two different locations. Their resolution and sensitivity to light are low and the beam profile cannot be clearly observed when the beam is lightly focused (see Fig. 3 showing typical pictures of CID cameras beam profiles). CCD cameras will be thus installed close to the emittance meter to provide a clear image of the beam in any experimental condition. They will be used during the commissioning phase with proton operation, whose radiation and induced activation at 100 keV is negligible.

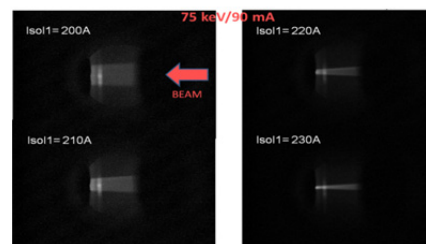


Figure 3: Deuteron beam profiles measured with CID cameras for different coil currents of the 1st solenoid.

The analysis of ion species fraction (such as D^+ , D_2^+ and D_3^+) is done by the Doppler Shift technique between the two solenoids of the LEBT, by means of a CDD camera installed with 20° angle to the focal plane of a monochromator. The weak radiation hardness of these devices is overcome with a 20 m long Fujikura radiation hard fiberscope to transport the fluorescence light from the vault to the monochromator located outside the accelerator vault. This last one is set to the wavelength of the D_α Balmer series (± 40 nm) to isolate the fluorescence coming only from the interaction of the beam with the

residual gas. Species fraction (spectroscopy), species fraction beam profile (imaging) and source impurities can then be analysed. Results of measurements from the commissioning at Rokkasho are reported elsewhere [11, 14].

Measurement of Space Charge Compensation

The high space charge of LIPAc, due to the low energy and high intensity beam, can be partially compensated in the LEBT when the beam interacts with the residual gas of D_2 [15, 16]. A Four Grid Analyser has been installed in the first diagnostic chamber of the LEBT in order to perform measurements of the beam potential well of the compensated beam, and to calculate the degree of space charge compensation. Either secondary electrons or D_2^+ ions can be analysed. The experimental space charge compensation values found using such a device for the 75 keV, 130 mA proton beam of the LEDA injector range from 95% to 99% [17]. It has been theoretically [18] and experimentally [19, 20, 21] observed that the beam emittance can be improved by injecting some heavy gas in the beam line, and that this improvement depends strongly on the gas species. During deuteron operation at Rokkasho, measurements of space charge compensation and of beam emittance have been performed with and without Krypton gas injected inside the LEBT [11].

EMITTANCE DATA ANALYSIS

Emittance Measurement Unit (EMU) that is used for the LIPAc injector is an Allison scanner [22] which can be installed either on the first or second diagnostic box. Its design has been optimized to sustain 15 kW of beam power in CW and for a critical beam diameter of 30 mm. It allows reconstituting the beam projection in the vertical plane of phase space. Emittance measurements are performed during the commissioning between the two solenoids to characterize the beam as close as possible to the source, and after the injection cone to characterize the beam at the entrance of the RFQ. Plans to measure the emittance in a third phase at the exit of the accelerator column are being discussed, but possibly are not needed if thorough understanding is being achieved during the last quarter of 2015.

The ECR source produces not only D^+ but also D_2^+ and D_3^+ molecular ions, with D^+ fraction ratio which should be of at least 80% with a suitable optimization of the source parameters. The extraction system has thus been optimized to extract a total beam current from 150 mA to 175 mA in order to be able to reach the required D^+ current of 140 mA at the energy of 100 keV at the RFQ entrance. A $\phi 12$ mm cone shaped with an angle equal to the D^+ beam theoretical convergence (half-angle of 8°) is installed just upstream the RFQ injection to stop the undesired particles, mainly D_2^+ and D_3^+ .

During the first stage of the commissioning phase, the Allison scanner has been installed between the two solenoids and the three species are thus still significantly present. Figure 4 shows raw data from the Allison scanner

for a deuteron beam of 91 mA/100 keV and in CW operation.

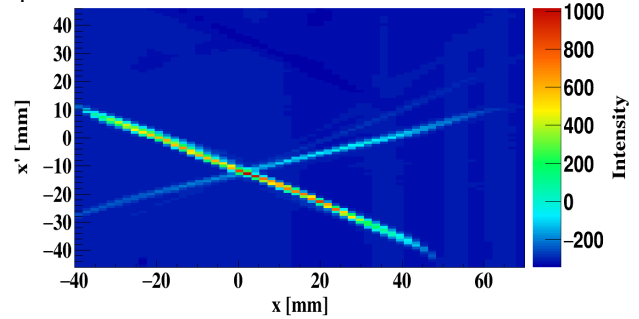


Figure 4: Raw data from the Allison scanner for a deuteron beam of 91 mA/100 keV and CW operation.

The two solenoid coil currents were set to maximize the beam transmission to the RFQ injection cone in order to be in the same condition than for the operation of the whole LIPAc. D^+ ion species are in this case convergent, as it can be observed on Fig. 4. D_2^+ and D_3^+ ion species diverge due to their higher magnetic rigidity and the three species are mixed on the beam axis (X -position = 0 mm). A high and non-homogeneous background is present in the data as described later in the article. In order to calculate the emittance of the desired species (i.e. D^+), D^+ spectrum needs to be isolated and the different steps are described below to perform this task automatically:

- Detection and removal of the background
- Detection and isolation of D^+ , D_2^+ , D_3^+ spectra
- In the area where the three species are mixed, interpolation of D_2^+ and D_3^+ spectra
- Subtraction of this interpolation to D^+ spectrum

Species fraction ratio can moreover be obtained by calculating the integrated intensity of each isolated species. An algorithm has been developed to perform these different steps automatically. The emittance and the D^+ fraction ratio can thus be obtained on-line for the beam tuning. Results of species fraction ratio measured with the Allison Scanner and the deported spectrometer have been compared [14].

Background Detection

The algorithm is written in Python [23] using ROOT [24] libraries (pyROOT). For background detection, the function member “Background” of the class “TSpectrum” of ROOT is used. It allows separating useless spectrum information (continuous background) from peaks, based on Sensitive Nonlinear Iterative Peak Clipping Algorithm [25, 26]. This function performs one-dimensional background estimation and it is used to detect background for each X -position of the Allison Scanner, i.e. for each abscissa of the emittance histograms. Its input parameters are optimized in order to remove only background and not real signal. Figure 5 shows a typical background detected by “TSpectrum” from the raw data shown on Fig. 4. A negative signal which seems to be homothetic to the beam can be clearly seen, probably due to secondary electrons produced inside the Allison scanner. Neutral particles

(due to beam neutralisation) can also be observed at the X-position of 20mm.

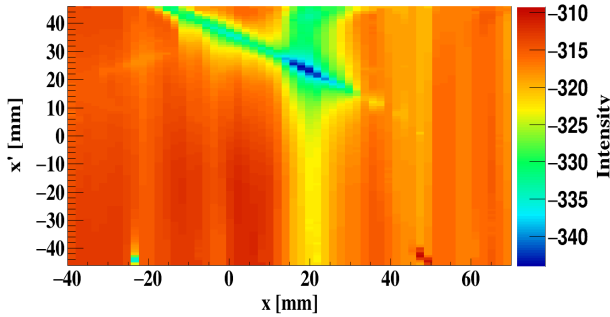


Figure 5: Typical background detected by “TSpectrum” from raw data of the Allison scanner shown on Fig. 4.

Ion Species Detection

Once the background has been detected and subtracted from the raw data, the algorithm can detect the three species. To perform this task, the function member “Search” of the class “TSpectrum” is used. It allows identifying one-dimensional peaks in a spectrum with the presence of continuous background and statistical fluctuations, i.e. noise. The algorithm is based on smoothed second differences that are compared to its standard deviations [25, 26].

Peaks detection of the three ion species are performed in one dimension, using this function at different X-positions where the different ion species are well separated. To make a matching between the peaks and the three ion species, several criteria are used depending on the X-position such as the highest intensity and the distance between peaks. A polynomial fit is then performed for each species using the identified peaks in order to identify the peaks at each X-position. For each species, pixels which do not have a null value around the polynomial fit are kept. A finer criterion using “TSpectrum” is applied to know the boundary between species when they are close to each other. On Fig. 6, peaks detections of the species are shown with their polynomial fits after background subtraction. D⁺, D₂⁺, D₃⁺ and H₂O can be clearly seen.

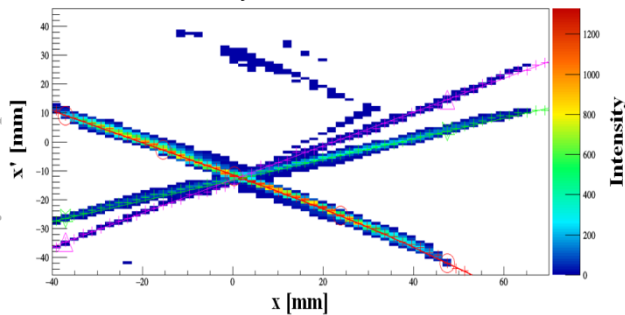


Figure 6: Peaks detections of D⁺, D₂⁺ and D₃⁺ ion species after subtracting the histogram background of Fig. 4.

Interpolation of D₂⁺ and D₃⁺ Ion Species

From the Scipy library of Python, a smooth bivariate spline approximation function of order 5 is used to perform the interpolation of D₂⁺ and D₃⁺ species in the

area where the three ion species are mixed. The data where D₂⁺ and D₃⁺ species are mixed are given to the interpolation function in order to perform the interpolation of both species in the same time. In fact, D₂⁺ and D₃⁺ species are mixed in a large position range and D₂⁺ and D₃⁺ species cannot be interpolated separately. This interpolation is then subtracted to the D⁺ species spectrum and the emittance of D⁺ species can be then calculated (see Fig. 7). First emittance results of the injector commissioning at Rokkasho, obtained with our method, are reported in [11].

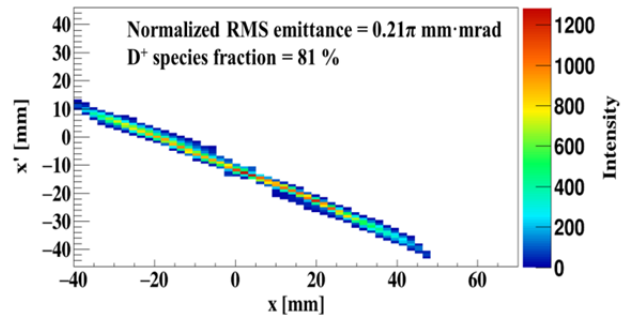


Figure 7: Example of an Histogram of D⁺ after interpolation subtraction.

Figure 8 shows the histogram of D₂⁺ after interpolation with the area where D₂⁺ and D₃⁺ are mixed. Figure 9 shows the histogram of D₃⁺ where the gap corresponds to the area where D₂⁺ and D₃⁺ are mixed. The calculation of D⁺ species fraction is performed as below:

$$D^+ \text{ species} = \frac{A1}{A1+A2+A3}$$

where A1 corresponds to the area of Fig. 7, A2 to the area of Fig. 8 and A3 to the area of Fig. 9.

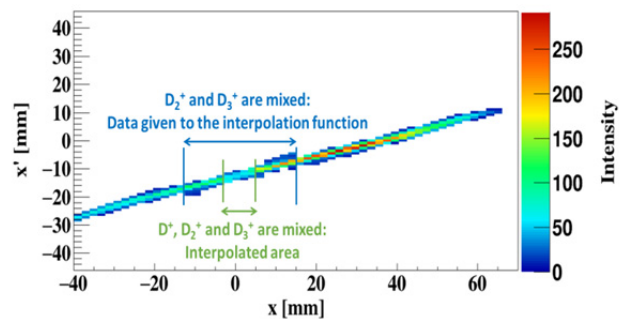


Figure 8: Histogram of D₂⁺ after interpolation.

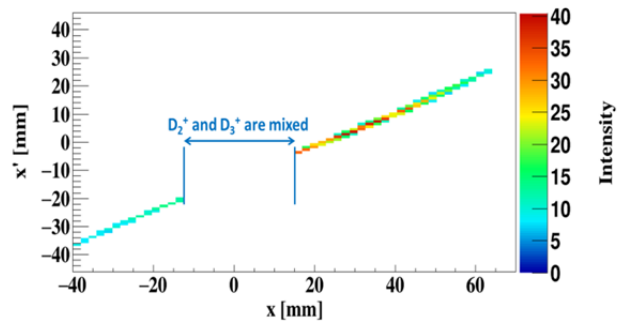


Figure 9: Histogram of D₃⁺ without interpolation.

Separation of the Ion Species Experimentally

The three species have been experimentally separated by setting the solenoids coil currents to a null value and by using instead the magnetic steerer which is integrated to the first solenoid. This experimental set-up can be seen as a kind of Wien filter [27]. Figure 10 shows an example of emittance data obtained between the two solenoids from the Allison scanner with such a set-up. The proton beam current was 90 mA for an energy of 50 keV. No interpolation needs thus to be done to analyse these data.

A second set-up has been performed without using the steerers but with the coil current of the first solenoid set to focus enough strongly H^+ species on the emittance meter to avoid large emittance aberrations coming from non-linear magnetic fields on the edge of the solenoid. Interpolation was thus included in the data analysis.

Emittance measurements have been performed with these two set-ups for different parameters of the injection source, implying a significant variation of the H^+ fraction ratio. The results of H^+ fraction and of emittance obtained with these two set-ups have been compared for each setting of the source parameters and show a difference of less than 1%. This gives a strong confidence on the accuracy of emittance measurements and analysis.

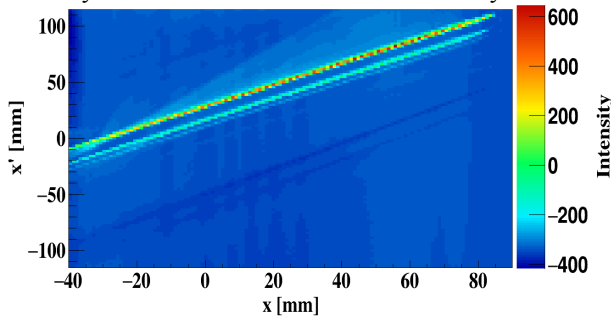


Figure 10: Raw data from the Allison scanner with the solenoids coil currents set to 0 A and with the magnetic steerer integrated to the first solenoid set to 150 A.

Test of the Algorithm Efficiency

Beam dynamics simulations [15, 18] have been performed with a 170 mA/50 keV proton beam. Emittance histograms have been obtained between the two solenoids for a normalized RMS emittance of 0.45π mm·mrad and for two different H^+ fraction ratios, i.e. 55% and 72%. Background detected with “TSpectrum” from arbitrary real measurements have been first multiplied by a fixed factor and then added to the simulated histograms. Figure 11 shows the histogram obtained for the H^+ fraction ratio of 55%.

The algorithm was used to calculate the emittance of the H^+ beam and the H^+ fraction ratio from these noisy simulations. The results were compared with the ones given by the simulations (before adding the background) and differences from less than 1% to a maximum of 4% have been observed. This shows that the background is accurately removed and that the interpolation accuracy is sufficient with this algorithm.

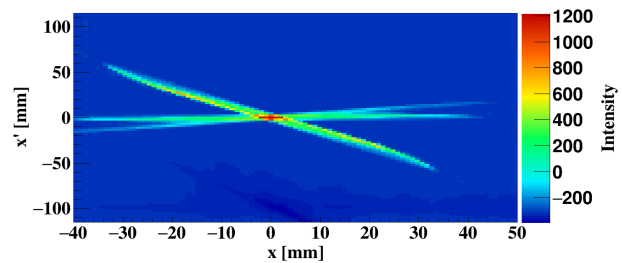


Figure 11: Emittance simulation between the two solenoids for a 170 mA/50 keV proton beam; RMS normalized emittance = 0.45π mm·mrad; H^+ ratio = 55%.

CONCLUSION

Beam diagnostics of the LIPAC injector have been commissioned at Rokkasho and are indispensable tools to achieve the required challenging beam characteristics at the RFQ entrance to allow CW operational mode. Modifications to enhance performance are planned such as the installation of a dipolar magnetic system to get a more accurate measurement of the beam current with the beam stoppers and the installation of CCD cameras during proton beam commissioning.

In order to analyse raw emittance data of high and non-homogenous background from an Allison scanner, an algorithm has been developed that allows both an automatic on-line calculation of the emittance rms values and of the species fraction ratio.

REFERENCES

- [1] J. Knaster et al, Nuclear Fusion 55 (2015) 086003.
- [2] J. Knaster et al, Proc. IPAC 2013, TUOAB101, Shanghai.
- [3] A. Mosnier et al, Proc. IPAC 2012, THPPP075, New Orleans.
- [4] R. Gobin et al, Proc. IPAC 2013, THPWO003, Shanghai.
- [5] M. Comunian et al, Proc. LINAC 2008, MOP036, Victoria.
- [6] H. Dzitko et al, Proc. IPAC 2015, THPF006, Richmond.
- [7] R. Gobin et al, Rev. Sci. Instrum., 79 (2008) 02B303.
- [8] N. Chauvin et al, Proc. IPAC 2013, THPWO006, Shanghai.
- [9] R. Gobin et al, Rev. Sci. Instrum. 85, 02A918 (2014).
- [10] R. Gobin et al, Proc. ICIS 2015, C151517-MonPS05, New-York, Rev. Sci. Instrum. (2016).
- [11] Y. Okumura et al, Proc. ICIS 2015, WEDM04, New-York, Rev. Sci. Instrum. (2016).
- [12] F. Senée et al, Proc. DIPAC 2011, TUPD46, Hamburg.
- [13] F. Senée et al, Proc. DIPAC 2009, TUPB14, Basel.
- [14] K. Shinto et al, Proc. ICIS 2015, C151669-ThuPS18, New-York, Rev. Sci. Instrum. (2016).
- [15] N. Chauvin et al, Proc. HB 2012, THO3A03, Beijing.
- [16] N. Chauvin et al, Rev. Sci. Instrum. 83, 02B320 (2012).
- [17] R. Ferdinand et al, Proc. PAC 1997, 6W010, Vancouver.
- [18] N. Chauvin et al, Proc. LINAC 2008, MOP072, Victoria.
- [19] R. Gobin et al, Rev. Sci. Instrum. 70 n° 6, 2652 (1999).
- [20] R. Hollinger et al, Proc. Linac 2006, TU3001, Knoxville.
- [21] P.-Y. Beauvais et al, Rev. Sci. Instrum. 71 (2000) 1413.
- [22] P.W. Allison et al, IEEE Trans. Nucl. Sci. NS-30, 2204-2206 (1983).
- [23] <https://www.python.org/>.
- [24] <https://root.cern.ch/drupal/>.
- [25] M. Morháč et al, NIM, A401 (1997) 113-132.
- [26] C. G Ryan et al, NIM, B34 (1988), 396-402.
- [27] D. Catana et al, Report WP10 IDRANAP 15-01/2001.